Eur. Phys. J. Plus (2021) 136:1115
https://doi.org/10.1140/epjp/s13360-021-02113-4

THE EUROPEAN PHYSICAL JOURNAL PLUS

Regular Article

The effect of outlet location on heat transfer performance in micro pin-fin cooling used for a CPU

Ferhat Koca[1,a], **Mustafa Zabun**[2,b]

[1] Faculty of Technology, Department of Automotive Engineering, Sivas Cumhuriyet University, 58140 Campus, Sivas, Turkey
[2] Faculty of Engineering, Department of Mechanical Engineering, Yeditepe University, İstanbul, Turkey

Received: 19 April 2021 / Accepted: 25 October 2021

Abstract In this study, the simulation of the coolant flow using micro-pin fins in the CPU heat sink was numerically presented with ANSYS-Fluent, a Computational Fluid Dynamics (CFD) program. Four different inlet–outlet configurations were employed in the heat sink. Keeping the inlet position of the flow to the heat sink fixed, the effects of the outlet position change on the pressure drop and thermal performance were examined. The flow field and heat transfer of each case were simulated with the SST k-ω turbulence model, three-dimensional study of steady, incompressible flow. In the study, a 2 mm diameter copper tube was used in the staggered arrangement fins array with the 0.23 porosity value. Reynolds number was in the range of $5000 < Re < 12{,}000$ and 2 kW/m^2 constant heat flux to the cooling base was taken into consideration boundary conditions. Velocity streamlines, TKE and temperature distributions, Nusselt number (Nu), skin friction values (f), pressure drop (ΔP), thermal resistance (R_{th}) and performance criterion (PEC) changes were presented to detail the hydrodynamic and thermal performance characteristics along the heat sink surface with the increase of Reynolds number. Results showed that as the Reynolds number increased, Nusselt number increased and skin friction decreased. In addition to the improvement in heat transfer for the finned models considered according to the finless cooler, the results show that the input–output configurations make a minimum difference of 32.25% in the performance criteria. The significance and novelty of this investigation consist in a consideration of an electronic devices cooling system, as well as an assessment of the influence of inlet/outlet configuration on the cooling process for a CPU.

List of symbols

A	Area
c_p	Specific heat at constant pressure, (kJ/kg K)
D_h	Hydraulic diameter, (mm)
f	Friction factor
H	Height of channel (mm) (see Fig. 1)

[a] e-mail: ferhatkoca@cumhuriyet.edu.tr (corresponding author)
[b] e-mail: mzabun@outlook.com

Published online: 08 November 2021

L	Length of the channel (see Fig. 1)
h	Heat transfer coefficient, (W/m^2 K)
k	Thermal conductivity (W/m K)
Nu	Nusselt number
P	Pressure, (Pa)
q”	Heat flux (W/m^2)
Re	Reynolds number
T	Temperature, (K, °C)
U_m	Mean velocity, (m/s)
w	Width (mm)
Rt	Thermal resistance
x, y, z	Cartesian coordinates
ρ	Density
μ	Viscosity, (Pa s)
s	Surface
avg	Average
SST	Shear stress transport
TKE	Turbulence kinetic energy

1 Introduction

Computers, with the rapid development of technology, have become indispensable elements of modern life, which are used in almost every field today, from education to health, from banking to aviation. In addition to increasing usage performance, they continue to be developed according to user demands such as smaller sizes, less power consumption and less noise-free operation. Studies such as increasing the information flow rate and dimensional miniaturization on computers cause serious temperature increases on microprocessors (CPU). In older microprocessor technologies, when the microprocessor temperature increased, the system would protect itself and often the computer would shut itself down. Nowadays, when the microprocessor temperature increases, it provides safe operation by changing the processor frequency. In short, as the temperature increases, the microprocessor decreases its operating frequency and performance losses begin. In other words, the performance at 90 °C and the performance at 30 °C are not the same. For this reason, CPU cooling is very important to have safe working conditions at the appropriate temperature. At this point, micro-pin fin heat sinks (MPFHS) are widely used to improve heat transfer.

In a micro-pin fin heat sink, it is managed with an expanded effective surface area for improved heat transfer, stimulation of the fluid mixture and disruption of the thermal boundary layer and optimum heat exchange [1].

Numerous experimental and numerical studies aim to explore the hydrothermal aspects of the finned heat sink, which depend on various factors including pin–fin morphology, arrangement, porosity and tip clearance, inter-fin spacing, flow rate, and dispersion [1–3]. A limited number of studies have combined thermal performance optimization of the micro-pin fin heat sink, utilizing nanofluidic coolers [4–6]. However, very few studies have been done on the adjustment of the fluid inlet / outlet cross sections as Hempijid and Kittichaikarn [7].

Peles et al. investigated the heat transfer and pressure drop phenomena on a series of micro-pin fins. They noted that the thermo-hydraulic performance of flow through the array of microscale cylindrical pin vanes was superior to flat micro-channel-based cooling. They recommended dense pin fin configurations to suppress convective thermal resistance at high

Reynolds numbers, and less frequent arrangements at low Reynolds numbers [8]. Qu and Siu-Ho conducted experiments to measure the pressure drop in a water-cooled two-phase miniature heat sink containing a series of stepped square micro-pin fins. They argued that two-phase micro-pin fin heat sinks provide better flow stability than their micro channel counterparts. They explained that the reason for this is that the interconnected nature of flow gates in micro pin-wing arrays encourages more stable biphasic flow [9].

Ambreen et al. investigated the thermo-hydraulic properties of Al2O3—Cu/water hybrid nano fluid in micro-pin fin heat sink. They used square, circular and elliptical fins. They compared the performances of heat sinks by obtaining log mean temperature difference, mean (Nu_{avg}) and surface (Nu_s) Nusselt number. They obtained Nu_{avg} increases of 25.14%, 19.65% and 24% for square, circular, and elliptical fins, respectively [10].

Chiu et al. quantitatively and experimentally investigated the liquid cooling efficiency of heat sinks containing micro-pin fins. They have applied the heat flux from the cooler base as 300 kW/m^2. They stated that the heat transfer performance depends on the porosity of the micro-pin blade array and pin diameter [11].

Yuan et al. performed numerical simulations of the effects of air velocity, pin diameter, pin array on the hydraulic and thermal performances of the pin fin heat sink (PPFHS) using Fluent 6.3.26 commercial software. They showed that pin height and air velocity have significant effects on the thermal hydraulic performances of the pin fin heat sink, and noted that the effects of PPFHS sequential/staggered array and adjacent pin downstream center distance were less remarkable [12].

Gong et al. studied the liquid flow and heat transfer numerically to reveal the thermal performance and cooling capacity of micro channel heat sinks [13].

Hamdi et al. conducted a comprehensive review of the methods used to optimize the hydrothermal design of heat sinks. They reviewed current research on passive and active techniques used to increase heat removal from heat sinks by varying either the solid area or the liquid area. They reported that it is still an interesting subject for researchers to increase the heat transfer rate of heat sinks investigated in many aspects [14].

As in the open literature, researchers basically argued that the heat transfer performance of a heat sink can be increased by properly designing the geometric parameters of the heat sink [15–18].

The aim of this study is to numerically examine the heat transfer effect of the coolant flow with the Computational Fluid Dynamics (CFD) program using a micro-pin fin heat sink. The designed heat sink has the dimensions of the heat sink used in a CPU mainboard chip. Studies in the literature focus on fin structures on the heat sink or the type of coolant. The results created by the inlet and outlet section position variations have not been determined by the researchers. In the present study, while the flow-inlet position is fixed, the effects of the outlet position change on pressure drop and thermal performance have been investigated. In the study, a 2 mm diameter copper tube was used in the staggered arrangement fins array with the 0.23 porosity value (fins area/plate area). Reynolds number was in the range of $5000 < Re < 12{,}000$ and 2 kW/m^2 constant heat flux to the cooling base was taken into consideration boundary conditions. Velocity streamlines, TKE and temperature distributions, Nusselt number, skin friction values, pressure drop, thermal resistance and performance criterion changes are presented to detail the hydrodynamic and thermal performance characteristics along the heat sink surface with the increase of Reynolds number.

2 Model description

The present study deals with forced convection heat transfer through a CPU. The main geometry used in the study carries the physical dimensions of a micro channel embedded in a high conducting solid, the same as used in the research conducted by Bhattacharyya et al. [19]. Figure 1 shows the micro channel volume where the micro-pin fins are placed and the micro-pin fin structure, which are used as the calculation area in this study, together with the CPU.

The basic geometric parameters of the models are shown in Fig. 2 and given in Table 1, respectively. The outer walls and the upper surface of the $L_1 \times W_1$ size micro channel were assumed to be adiabatic. Below the occupied area of the pin fins, the base of the heat sink ($L_2 \times W_1$) is subjected to a constant heat flux density of 2 kW/m^2. Directed by the inlet section, the water used as the cooling flows over the micro pins before leaving the outlet section. Flow was evaluated in the Reynolds number range of $5000 < Re < 12{,}000$, depending on the pin hydraulic diameter [20, 21]. In addition to different Re numbers, thermal performance was examined for 4 different positions of the micro channel outlet section as shown in Fig. 3. For comparison, the computational area and all relevant dimensions of the heat sink are consistent with an experimental study [11] based on a water-cooled chiller with circular micro-pin fins.

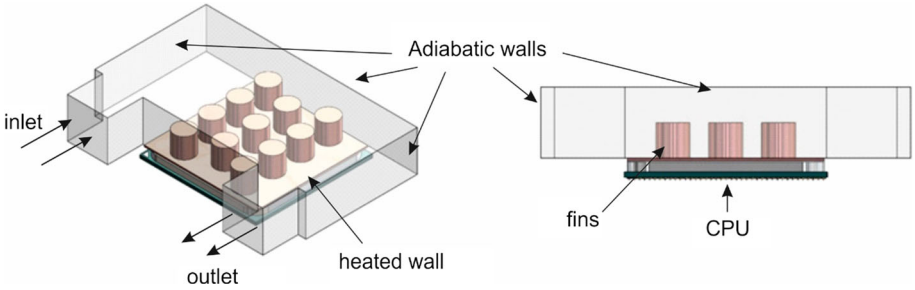

Fig. 1 View of micro channel (heat sink), and micro pin fins placed on the CPU

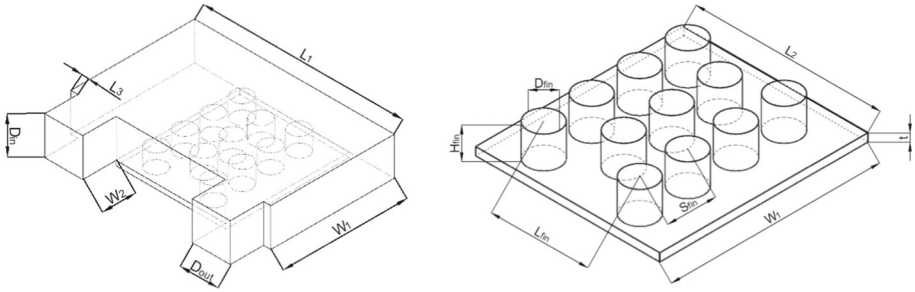

Fig. 2 Micro channel and fins dimensional view

Table 1 Dimensions of the modeled micro pin–fin heat sink

Parameter	L_1	L_2	L_3	L_{fin}	W_1	W_2	H_1	H_{fin}	S_{fin}	$D_{in} = D_{out}$	D_{fin}	t
Dimension (mm)	21	11.5	0.75	6	13	3.5	4	2	3	4 × 4	2	0.5

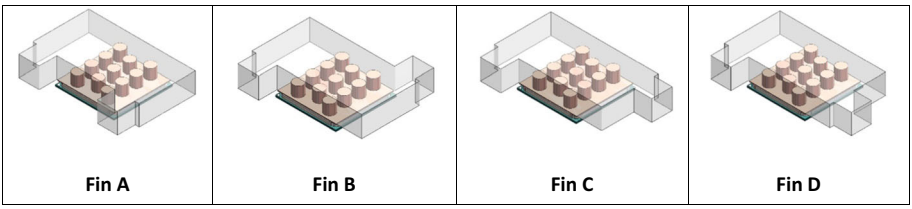

Fig. 3 View of different micro channel structures used in the study according to the exit section position

Four different models used in the study are given in Fig. 3. While designing the models, the coolant inlet cross section was kept fixed, and the position of the outlet section was changed. Fin A is the model of the fluid inlet and outlet section positions located on the same plane, Fin B is the model of the inlet and outlet positions located diagonally on a 180° opposite plane, Fin C is the distant model of the inlet and outlet positions in 90° mutual plane, Fin D represents the 90° close-up pattern of the inlet and outlet positions.

3 Mathematical formulation

As shown in the geometric model (Fig. 1), both the liquid and solid region were used in the simulation of the micro-pin finned heat sink. The standard k-ω turbulence model was adopted to describe the turbulent fluid flow in the forced convection heat transfer analysis. Mass, momentum and energy government equations are set as follows [13]:

$$\nabla.(\rho u) = 0 \tag{1}$$

$$u.\nabla(\rho u) = -\nabla p + \mu\nabla^2 u \tag{2}$$

$$u.\nabla T = k.\frac{\nabla^2 T}{\rho c_{\mathrm{p}}} \tag{3}$$

The working fluid used in all conditions was water and its thermodynamic properties were as follows: $\rho = 998{,}2$ kg/m^3, $c_{\mathrm{p}} = 4182$ J/(kg K), k = 0.6 W/(m K), $\mu = 0.001003$ kg/(ms), where ρ, c_{p}, k and μ mean density, specific heat, thermal conductivity and viscosity, respectively.

Several assumptions have been used to make the problem more plausible and simple. These assumptions are listed below:

- Flow is constant, uniform and turbulent,
- There is no change in thermo-physical properties with temperature (used only in model comparisons in numerical studies to shorten the analysis time),
- Fluid is incompressible and viscous,
- There is no slip condition on the walls
- Bi-directional connection has been considered for solid–liquid regions and heat transfer by radiation has been ignored.
- The refrigerant has a temperature of 300 K at the inlet and has fully developed velocity profile.

4 Numerical details and boundary conditions

All micro-fin channel simulation was done with commercial software, ANSYS-Fluent. Mesh structure with tetragonal cells was used for the models. In order to obtain accurate and precise results, more dense mesh has been applied to the boundary walls and areas close to the fin surfaces. In addition, 20-layer inflation was used on fin surfaces and the contact surfaces of the control volume with the fin surface. The discretization scheme was set as Second Order Upwind for momentum, COUPLED for numerical scheme and second order analysis. Turbulence density was determined as 0.5%. The flow rate in all solid walls was set to zero. Micro channel outer solid walls were arranged to be adiabatic. In the calculation, the convergence criteria between two consecutive iterations were set to be less than 1×10^{-3} relative deviation for velocity and continuity, and less than 1×10^{-6} for the solution in the energy equation. Nusselt number and skin friction coefficient were determined as output parameters to ensure mesh independence and first analyzes were obtained. The results obtained according to the number of meshes are given in Table 2 and their graphical form is presented in Fig. 4 to understand the change and determine the appropriate mesh number. The change of Nu number and skin friction values for mesh element number 156×10^3 and above is at acceptable levels. Considering the analysis time, analyzes were started with 200×10^3 mesh element numbers. In Fig. 5, the detailed view of the mesh structure determined and used by the mesh independence is given.

After post-processing the analysis results, the thermal resistance R_{th} [11], the average Nusselt number (Nu_{avg}) [1] and the surface Nusselt number (Nu_s) distribution are estimated by the following expressions:

Table 2 Average Nusselt number and skin friction values according to mesh element number

Mesh element	Nusselt	Skin friction
90,343	46.62	0.0108402
95,129	44.20	0.0103995
107,218	43.60	0.0107159
122,768	42.93	0.0110298
156,689	42.16	0.0120747
262,878	41.80	0.0128335
295,138	41.90	0.0129335

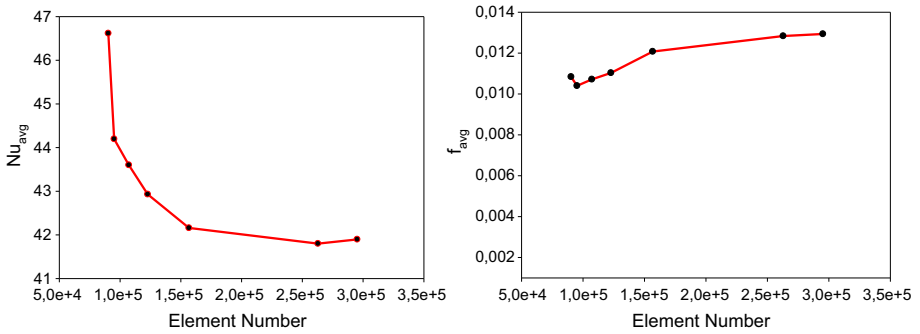

Fig. 4 Average Nu and friction change depending on mesh number

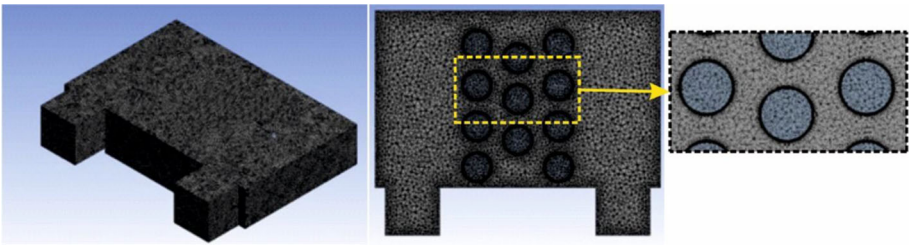

Fig. 5 Micro channel mesh structure view

$$R_{\text{th}} = \frac{T_{\text{b}} - T_{\text{in}}}{Q^{"}} \tag{4}$$

$$\text{N}u_{\text{avg}} = \frac{h_{\text{avg}} * S_{\text{fin}}}{k} \tag{5}$$

$$\text{N}u_{\text{s}} = \frac{h_{\text{s}} * S_{\text{fin}}}{k} \tag{6}$$

In Eq. (4), T_{b} and T_{in} are the heat sink base and coolant inlet temperatures, respectively. The average and local convective heat transfer coefficients (h_{avg} and h_{s}) in Eqs. (5) and (6) are, respectively, determined by the following equations [1]:

$$h_{\text{avg}} = \frac{h_{\text{fin}} A_{\text{fin}} + h_{\text{b}} A_{\text{b}}}{A_{\text{fin}} + A_{\text{b}}} \tag{7}$$

$$h_s = \frac{Q^{"}}{T(z)_{\text{s}} - T(z)_{\text{m}}} \tag{8}$$

A_{b} and A_{fin} given in Eq. (7) represent the total base wet surface area and fin surface areas, respectively.

Figure 6 shows the validation of the present study with the existing study in the literature. Validation of the CFD results used was performed by comparing them with analytical results

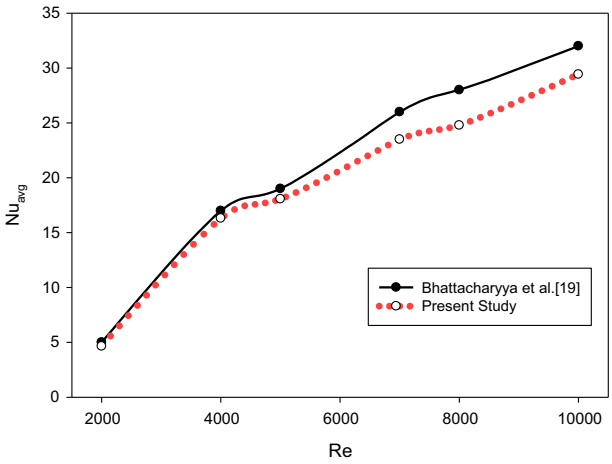

Fig. 6 Validation of the CFD results

from research conducted by Bhattacharyya et al. [19], which analyzed the performance of a cylindrical pin–fin heat sink in turbulent forced convection. The comparison contains the results obtained for the heat sink without fin. The Re-Nu solution curves were in good agreement with a maximum deviation of less than 8% as shown in Fig. 6. The slight difference after Re > 4000 is due to the increase in turbulence effects depending on the turbulence intensity used in the analyses. This shows that the accepted numerical results after mesh independence of the presented study are reliable.

5 Results and discussions

Four different flow-inlet velocities (u_{in}) of 1.25, 2, 2.512 and 3.01 m/s, corresponding to the Re numbers 5000, 8000, 10,000 and 12,000, respectively, were adopted to analyze their thermal and hydraulic performances in the micro-fin channel for four different output positions. The resulting streamlines and TKE distributions are given in Fig. 7 for Re = 5000, in Fig. 8 for Re = 8000, in Fig. 9 for Re = 10,000, and in Fig. 10 for Re = 12,000. The circulation of the coolant flow in the micro channel heat sink and its contact on the fin surfaces are factors that directly affect the heat transfer. It is clearly seen that the location of the outlet section directly affects this situation when the figures are examined. The flow circulation in the channel is more in the Fin A and Fin D models than the Fin B and Fin C models and also, the fluid tends to exit directly in Fin B and Fin C models. In all models and all Re numbers, a large vortex have occurred at the corner of the micro channel in the direction of the inlet section.

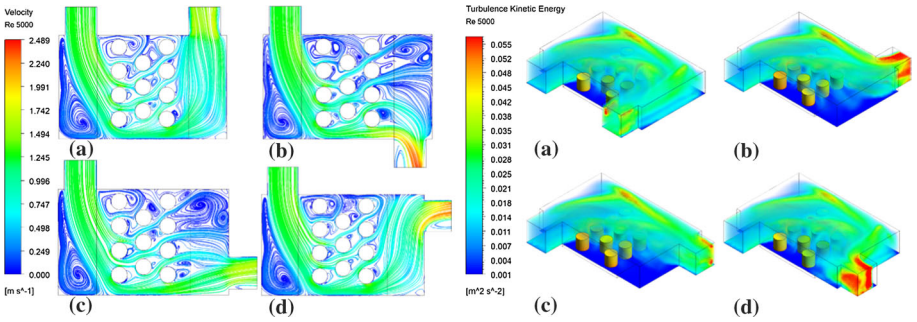

Fig. 7 Streamline and TKE distributions for Re = 5000 **a** Fin A **b** Fin B, **c** Fin C, **d** Fin D

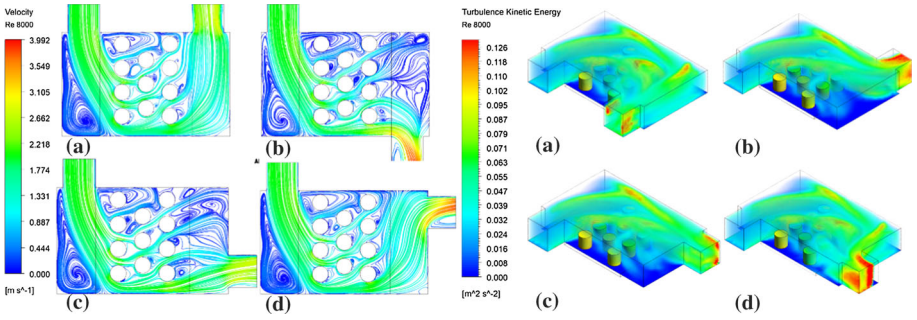

Fig. 8 Streamline and TKE distributions for Re = 8000 **a** Fin A **b** Fin B, **c** Fin C, **d** Fin D

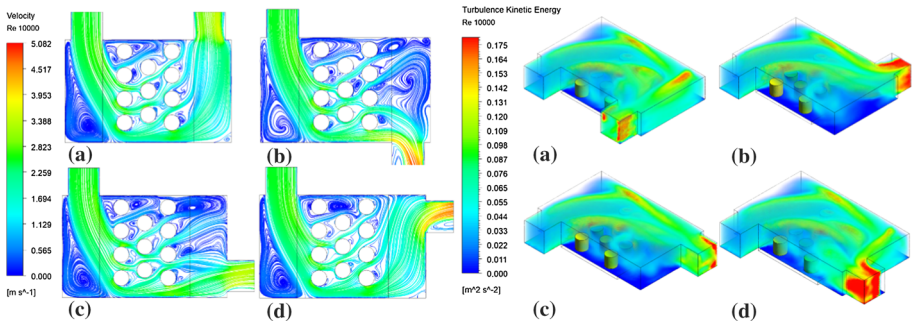

Fig. 9 Streamline and TKE distributions for Re = 10,000 **a** Fin A **b** Fin B, **c** Fin C, **d** Fin D

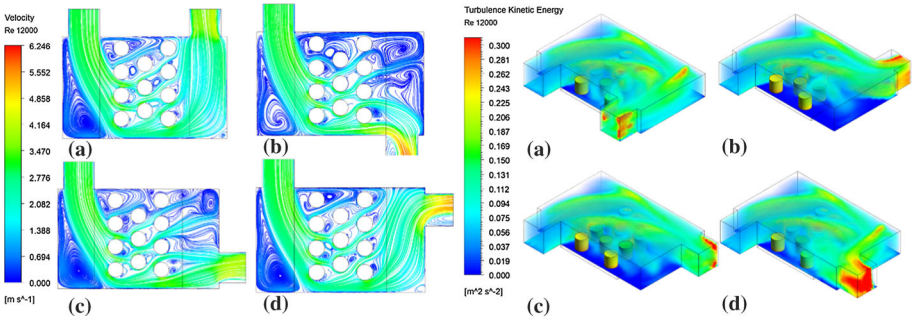

Fig. 10 Streamline and TKE distributions for Re = 12,000 **a** Fin A **b** Fin B, **c** Fin C, **d** Fin D

In the Fin B and Fin C models, in addition to these vortices, vortex regions were formed at the opposite diagonal corner of the micro channel. As can be clearly seen in the TKE images, the fluid circulation is minimal over the fins in the region close to the inlet cross section plane. Therefore, heat transfer through these fins is at the lowest levels. This region with the least refrigerant circulation is larger in Fin B and Fin C compared to Fin A and Fin D models. When the exit sections of the models are examined, it is revealed that both the velocity streamline and TKE values are higher in Fin B and Fin D models. This leads to the conclusion that the pressure drop in these two models is greater than in the other models.

Linear surfaces have been assigned between the fins, as shown in Fig. 11, in order to understand how the heat transfer changes along the surface through the heat sink plate placed

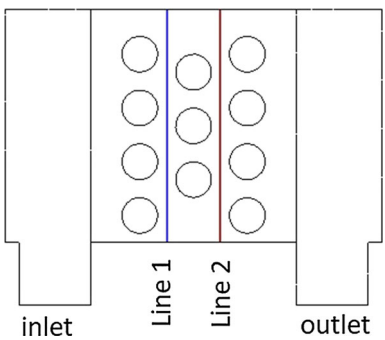

Fig. 11 View of Line 1 and Line 2 locations

on the CPU. The linear surface in the region close to the inlet section was named as Line 1 and the other as Line 2. Along the Line 1 and Line 2, the surface Nusselt and surface skin friction values were obtained over the dimensionless distance x/L.

In Fig. 12, the graph of surface Nusselt (Nu_s) changes obtained along Line 1 for models with different outlet section locations and micro channel without fin is given. As predicted, the surface Nu values is the lowest in the model called No Fin in the graph, since the heat transfer through the plate without the fin is the least. Nu_s changes of the models along the Line 1 surface follow an up and down path. This situation is caused by the difference in the fin wake region and the middle regions of the heat transfer of the fluid, which is directed from the channel inlet to the outlet, through the plate. In addition, the surface Nu values increase along the x distance in all models. The Nu_s changes given for Line 2 in Fig. 13 increases along the distance x as in Line 1, but the difference between instantaneous increase and decrease is smaller.

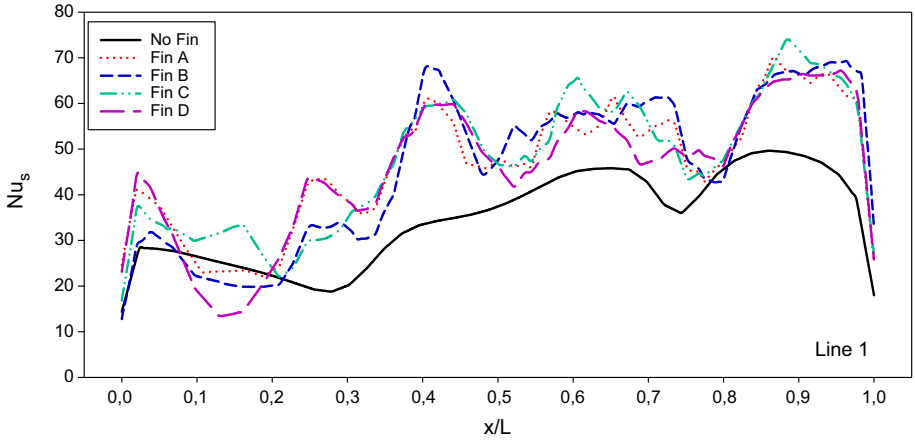

Fig. 12 Surface Nusselt number (Nu_s) along Line 1 (x/L)

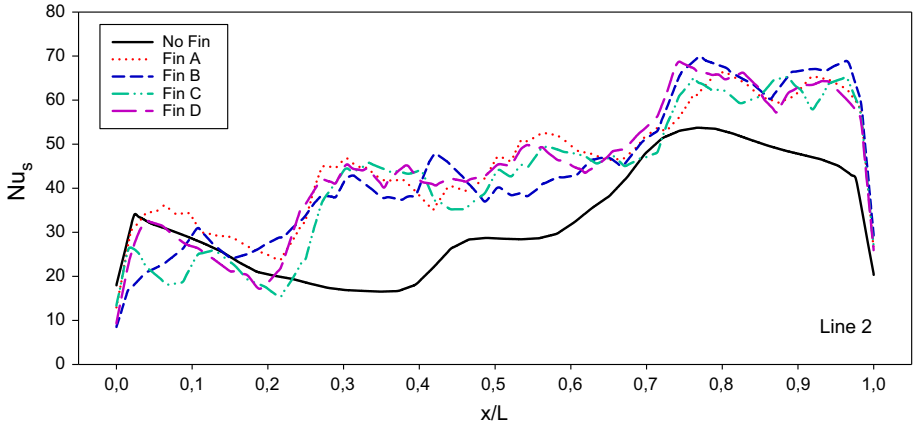

Fig. 13 Surface Nusselt number (Nu_s) along Line 2 (x/L)

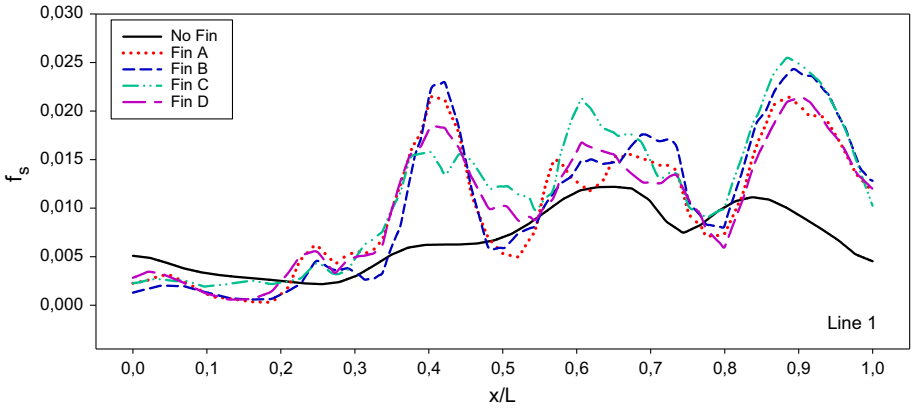

Fig. 14 Surface skin friction number (fs) along Line 1 (x/L)

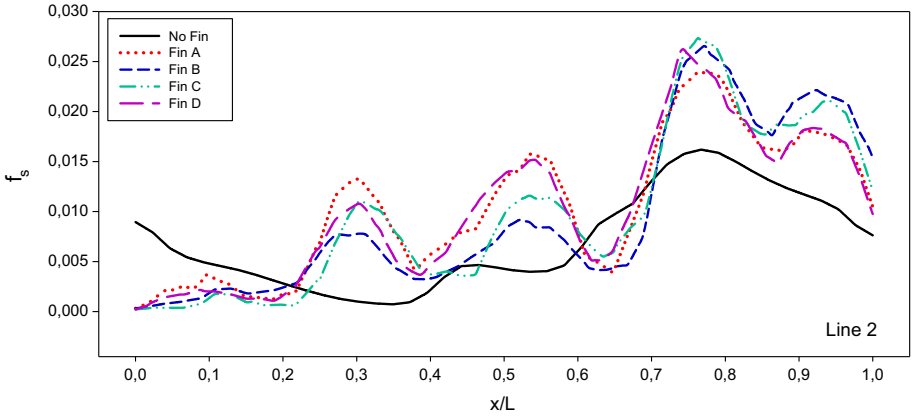

Fig. 15 Surface skin friction number (fs) along Line 2 (x/L)

Surface friction factor (f_s) changes are given along Line 1 in Fig. 14 and along Line 2 in Fig. 15. While the lowest surface friction factor occurs for the model without fins, the changes in the models with fins differ as in the surface Nu values, but increase with the distance x.

The dimensionless Reynolds (Re) number plays an important role in predicting the behavior of a fluid. Technically, the Re number is the ratio of inertial forces to viscous forces. With increasing this ratio (increasing the Re number), the flow velocity, flow turbulence, and turbulence kinetic energy increase and creates some effects on the fluid. Figure 16 shows the effects of Re number on pressure drop, average Nu number, average skin friction value, thermal resistance and PEC value. In the range of Re, 5000 to 12,000 values were taken in the study. Accordingly, it is clearly seen in Fig. 16a that the pressure drop increases in all models with the increase in the Re number. This is due to the fact that the flow becomes more turbulent as the flow velocity increases. This increase is greater in Fin B and Fin D models than the others. While the lowest pressure drop is seen in the model without fins, close parallelism is observed in Fin A and Fin C to the model without fins. This indicates that there is more energy loss between the inlet and outlet in Fin B and Fin D models, and therefore more pumping power is required with increasing Re number in these models.

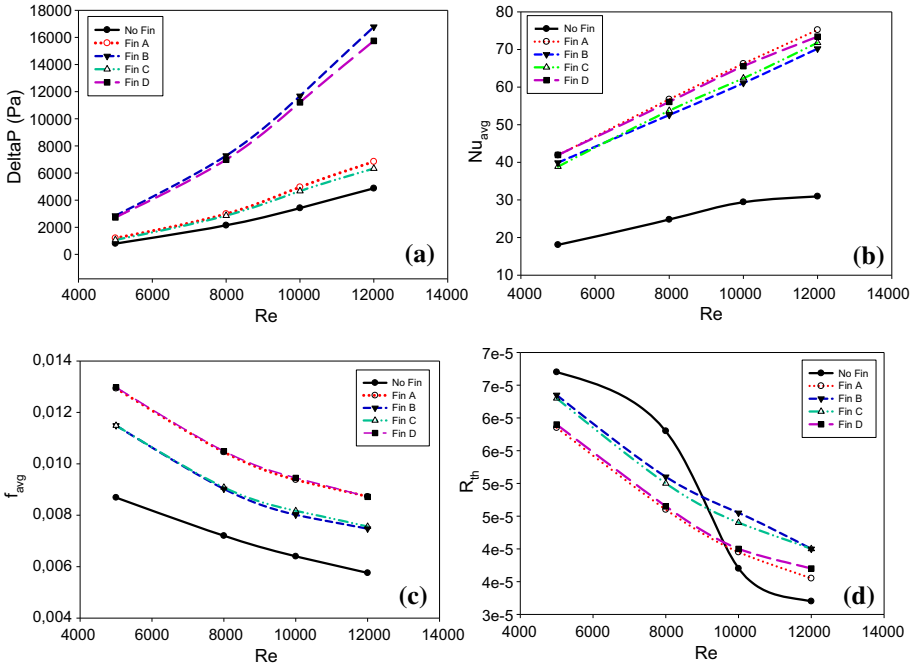

Fig. 16 Effect of Reynolds (Re) number on **a** pressure drop, **b** average Nu number, **c** average skin friction value **d** thermal resistance

Figure 16b gives the average Nusselt number changes with increasing Reynolds number. As is well known, Nusselt number for a flow system gives basic difference between convection and conduction heat transfer. For a relative low Nusselt number indicates conduction heat transfer dominates convective heat transfer, whereas for a large Nusselt number implies convective term dominant. This significance enables to design more efficient thermal engineering systems. In Fig. 16b, Nu_{avg} values increase with increasing Re number. This is due to the convection heat transfer increasing with the flow rate. There is a distinct difference in all models compared to the model without fins. The highest values are obtained for the Fin A model. These values are also given in Table 3.

Figure 16c shows the average skin friction change with increasing Reynolds number. The skin friction coefficient is a dimensionless skin shear stress which is nondimensionalized by

Table 3 Nu_{avg} and f_{avg} values obtained at different Re numbers

	No Fin		Fin A		Fin B		Fin C		Fin D	
Re	Nu_{avg}	f_{avg}	Nu_{avg}	f_{avg}	Nu_{avg}	f_{avg}	Nu_{avg}	f_{avg}	Nu_{avg}	f_{avg}
5000	18.06	0.0086	41.89	0.0129	39.90	0.0115	38.85	0.0115	41.95	0.0129
8000	24.78	0.0072	56.73	0.0104	52.57	0.0090	53.73	0.0091	56.07	0.0105
10,000	29.42	0.0064	66.21	0.0094	61.05	0.0080	62.35	0.0082	65.56	0.0095
12,000	30.95	0.0058	75.21	0.0087	70.22	0.0074	71.79	0.0076	73.41	0.0087

the dynamic pressure of a free flow. This coefficient is a function of shear stress on the wall, the density of fluid, and flow velocity. In all models, friction values decrease with the Re number. This reduction is due to the shear-thinning efect of power-law fuids. The friction values are the lowest as predicted for the model without any fin barriers. In Fin B and Fin C models, where the direction of the coolant from the inlet to the outlet is easier, the friction values are lower than the Fin A and Fin D models, where the fluid circulation is more.

Figure 16d shows the effect of increasing Reynolds number on thermal resistance. Thermal resistance is a material's resistance to heat as a measure of temperature difference and is the reciprocal of thermal conductivity. While the thermal resistance decreased with a similar slope in all models with the number of Re, it decreased sharply after Re = 8000 in the model without fin.

The increase in pressure drop is related to the increase of heat transfer. Therefore, it is very important to explain the efficiency of a cooling surface using performance evaluation criteria (PEC). Higher PEC values provide higher heat transfer. Furthermore, a PEC value greater than 1 indicates that the heat transfer rate is greater than the increase in pressure drop [22–24]. PEC values were obtained by the Eq. 9:

$$\mathrm{PEC} = \frac{\mathrm{Nu}/\mathrm{Nu_o}}{f/f_o{}^{(1/3)}} \tag{9}$$

Here *N*u and f represent the mean Nusselt number and average skin friction coefficient values for the evaluated surface with fins, while $\mathrm{Nu_o}$ and $\mathrm{f_o}$ represent the mean Nusselt number and average skin friction coefficient value for the straight surface without fins.

The effect of micro fins with different micro channel heat sink models on PEC is shown in Fig. 17 for different Re numbers. PEC values vary with increasing Re number due to Nu number and skin friction effect. According to PEC values, the most effective model is Fin A, and the least efficient model is Fin D. In other words, convectional heat transfer increased, shear stress decreased with the increase of flow rate in Fin A, while the ratio between these two was higher compared to other models.

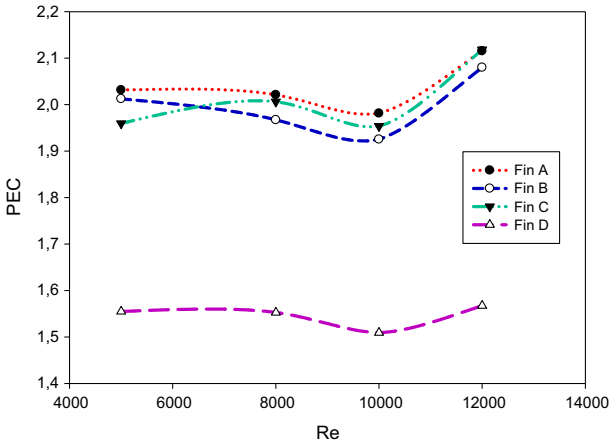

Fig. 17 The effect of Re number on PEC values

6 Conclusion

The varying of the fin number, fin geometry, channel shape, channel aspect ratio, grooved channel, inlet/outlet location, and ribs and turbulators in between channels have an attractive effect for getting the optimal thermal design of the heat sinks. In this study, the effect of micro-pin fins (MPF) used for CPU cooling on hydrodynamic and thermal performances with the change of micro channel fluid outlet position was investigated. This has affected the flow circulation over the existing cross-sectional areas of the MPF and thus the amount of heat transfer through the MPFs. The validity of the numerical model has been verified by comparing it to the datas of Bhattacharyya et al. [19]. The effects of the inlet/outlet configuration, and Reynolds number on pressure drop, temperature distribution, heat transfer performance, and outlet temperature have been presented. The findings of this study can be summarized as follows:

- Re number is an important flow parameter in MPFHS performance. As the Re number increases, the flow resistance will increase significantly and the thermal resistance and profit factor will decrease significantly.
- An increase in pressure drop occurred with the increase of Re number in all models. These pressure drops were greater in the Fin B and Fin D models and their value was higher with the Re number. In Fin A and Fin C models, it was less and closer to the finless model.
- Average Nusselt values in all models were found to be approximately 30% higher than the model without fins. The highest values occurred in Fin A, Fin D, Fin C and Fin B, respectively. Also, Nu numbers increase with the increase of Re number.
- The average skin friction factor, which is considered to be one of the factors leading to the pressure drop, decreases with the number Re and the lowest values were obtained for the model without fins, as predicted. The highest f_{avg} values were seen for Fin A and Fin D, while the lowest values were seen for Fin B and Fin C.
- Thermal resistances of MPFs against the heat transferred from the CPU decreased with the increase of flow rate.
- Performance criteria (PEC) values, which are the most important indicators of the efficiency of the models, have been calculated, it is clear that all models provide a more effective cooling compared to the finless model with the PEC > 1 value. However, the Fin D model has a lower PEC value than other models. The Fin A, Fin B, and Fin C models changed similarly with the increasing number of Re. However, for improved micro channels, the most effective model for cooling electronic components with a heat flux of 2000 Watt per square meter was found to be the Fin A model.
- Consequently, it shows that besides the improvement in heat transfer for the four models with fins, which were considered according to the finless heat sink, the results indicate that the inlet-output configurations create a min 32.25% difference in the performance criterion.
- Additionally, one of the world's largest companies, Intel, provided microprocessors for computer system manufacturers; gives importance to the issue of more heat removal from smaller areas with liquid or air cooling methods. This situation shows that the study will contribute to the literature.

References

1. J.F. Tullius, T.K. Tullius, Y. Bayazitoglu, Optimization of short micro pin fins in minichannels. Int. J. Heat Mass Transf. **55**(15–16), 3921–3932 (2012)

2. Y.K. Prajapati, Influence of fin height on heat transfer and fluid flow characteristics of rectangular microchannel heat sink. Int. J. Heat Mass Transf. **137**, 1041–1052 (2019)
3. G.V. Kewalramani, G. Hedau, S.K. Saha, A. Agrawal, Study of laminar single phase frictional factor and Nusselt number in In-line micro pin-fin heat sink for electronic cooling applications. Int. J. Heat Mass Transf. **138**, 796–808 (2019)
4. T.H. Tsai, R. Chein, Performance analysis of nanofluid-cooled microchannel heat sinks. Int. J. Heat Fluid Flow **28**(5), 1013–1026 (2007)
5. C.J. Ho, L.C. Wei, Z.W. Li, An experimental investigation of forced convective cooling performance of a microchannel heat sink with Al2O3/water nanofluid. Appl. Therm. Eng. **30**(2–3), 96–103 (2010)
6. M.I. Hasan, Investigation of flow and heat transfer characteristics in micro pin fin heat sink with nanofluid. Appl. Therm. Eng. **63**(2), 598–607 (2014)
7. T. Hempijid, C. Kittichaikarn, Effect of heat sink inlet and outlet flow direction on heat transfer performance. Appl. Therm. Eng. **164**, 114375 (2020)
8. Y. Peles, A. Kos, C. Mishra, C. Kuo, B. Schneider, Forced convective heat transfer across a pin fin micro heat sink. Int. J. Heat Mass Transf. **48**, 3615–3627 (2005)
9. W. Qu, A. Siu-ho, Measurement and prediction of pressure drop in a two-phase micro-pin-fin heat sink. Int. J. Heat Mass Transf. **52**(21–22), 5173–5184 (2009)
10. T. Ambreen, A. Saleem, S.A. Shehzad, C. Woo, Performance analysis of hybrid nano fluid in a heat sink equipped with sharp and streamlined micro pin- fins. Powder Technol. **355**, 552–563 (2019)
11. H. Chiu, R. Hsieh, K. Wang, J. Jang, C. Yu, The heat transfer characteristics of liquid cooling heat sink with micro pin fi ns. Int. Commun. Heat Mass Transf. **86**, 174–180 (2017)
12. W. Yuan, J. Zhao, C.P. Tso, T. Wu, W. Liu, T. Ming, Numerical simulation of the thermal hydraulic performance of a plate pin fi n heat sink. Appl. Therm. Eng. **48**, 81–88 (2012)
13. L. Gong, J. Zhao, S. Huang, Numerical study on layout of micro-channel heat sink for thermal management of electronic devices. Appl. Therm. Eng. **88**, 480–490 (2015)
14. H.E. Ahmed, B.H. Salman, A.S. Kherbeet, M.I. Ahmed, Optimization of thermal design of heat sinks: a review. Int. J. Heat Mass Transf. **118**, 129–153 (2018)
15. D. Sahel, L. Bellahcene, A. Yousfi, A. Subasi, Numerical investigation and optimization of a heat sink having hemispherical pin fins. Int. Commun. Heat Mass Transf. **122**, 105133 (2021)
16. A.A. Hussain, B. Freegah, B.S. Khalaf, H. Towsyfyan, Numerical investigation of heat transfer enhancement in plate-fin heat sinks: effect of flow direction and fillet profile. Case Stud. Therm. Eng. **13**, 2019 (2018)
17. X. Wang, M. Chen, D. Tate, H. Rahimi, S. Zhang, Numerical investigation on hydraulic and thermal characteristics of micro latticed pin fin in the heat sink. Int. J. Heat Mass Transf. **149**, 119157 (2020)
18. Y. Wang, K. Zhu, Z. Cui, J. Wei, Effects of the location of the inlet and outlet on heat transfer performance in pin fin CPU heat sink. Appl. Therm. Eng. **151**, 506–513 (2019)
19. S. Bhattacharyya, B. Souayeh, A. Banerjee, R. Sarkar, Numerical analysis of micro-pin-fin heat sink cooling in the mainboard chip of a CPU. Eur. Phys. J. Plus **123**, 1–10 (2020)
20. N. Sahiti, A. Lemouedda, D. Stojkovic, F. Durst, E. Franz, Performance comparison of pin fin in-duct flow arrays with various pin cross-sections. Appl. Therm. Eng. **26**(11–12), 1176–1192 (2006)
21. H.R. Seyf, M. Feizbakhshi, Computational analysis of nanofluid effects on convective heat transfer enhancement of micro-pin-fin heat sinks. Int. J. Therm. Sci. **58**, 168–179 (2012)
22. O. Manca, S. Nardini, D. Ricci, A numerical study of nano fl uid forced convection in ribbed channels. Appl. Therm. Eng. **37**, 280–292 (2012)
23. A. Pina, P. Ferrão, J. Fournier, B. Lacarrière, O. Le Corre, Heat transfer enhancement of a molten salt parabolic trough solar receiver with concentric and eccentric pipe inserts. Energy Procedia **142**, 624–629 (2017)
24. R.L. Webb, N.Y. Kim, *Enhanced Heat Transfer* (Taylor and Francis, NY, 2005)